

Optical feedback interferometry for sensing application

Thierry Bosch*

Noël Servagent

Ecole des Mines de Nantes
Department of Automatic Control and
Production Systems
4 rue Alfred Kastler
P.O. Box 20 722
44 307 Nantes Cedex 3
France
E-mail: bosch@len7.enseeiht.fr

Silvano Donati

Università di Pavia
Dipartimento di Elettronica
Pavia, Italy
E-mail: donati@ele.univ.it

Abstract. We review laser diode feedback interferometry as a general tool for sensing applications. After outlining the basic principles and the theoretical approaches used to describe the phenomenon, we present a few selected examples of applications in interferometry, as developed by various groups in recent years, such as a displacement sensor, a velocimeter or vibration sensor, and an absolute distance meter or range finder and angle sensor. Experimental results are also reported as an illustration. © 2001 Society of Photo-Optical Instrumentation Engineers. [DOI: 10.1117/1.1330701]

Subject terms: optical feedback; semiconductor lasers; sensors; displacement measurement; laser ranging.

Paper DDM-11 received July 24, 2000; accepted for publication July 24, 2000.

1 Background

Soon after the discovery of the laser, back-reflection was recognized as a serious source of disturbance, strongly affecting both amplitude and frequency of the laser oscillating field. The problem was studied by Nobel Prize winner Lamb, Jr., who in 1971 published two seminal papers (Spencer and Lamb^{1,2}) on self- and mutual-injection, revealing that amplitude and frequency modulations of the perturbed laser are generated in the back-reflection regime, proportional to the in-phase and in-quadrature components of the external field injected into the laser cavity. From one side, this work fostered the researches on injection-locking³⁻⁵ and synchronization phenomena⁶ in laser sources, with applications to master-slave lasers as well as to the newly developed ring-laser gyroscope;⁷ from the other side, it led to an improved understanding of the back-reflection phenomena and their control in optical fiber communications when using narrow-line lasers.⁸⁻¹⁰

Meanwhile, the application of feedback-induced phenomena to the detection of weak signals and to the optical pathlength of a remote reflecting target started to flourish. Perhaps, the first reported experimental result of operation by feedback interferometry is that of Rudd,¹¹ who in 1968 was able to detect a Doppler-shifted backscattered signal with a He-Ne laser tube. Then, the weak signal from a CD trace was read¹² by a diode laser-feedback mixer in 1975. The first example of full, up-and-down fringe counting with a feedback interferometer was reported¹³ in 1978, pointing out that the AM and FM driving terms contain just the sine and cosine of the external *phaseshift* $\Phi = 2kz$, while the root mean square sum of the modulated signal is proportional to the *amplitude* E of the detected field. A coherent 3D imaging system based on self-detection was reported by de Groot and Gallatin.¹⁴

Today, we may recognize a feedback interferometer (or a self-mixing or an injection interferometer etc., all are synonymous terms) as a system performing a special type of detection, the so-called *injection detection*,¹⁵ which is the optical counterpart of the superheterodyne detection well known in the radio waves technique. Injection detection is a special type of coherent detection,¹⁵ and like it has the advantage of always working at the quantum limit of the incoming signal as well as of being eventually homodyne (the self-mixing scheme) or heterodyne (the synchronization scheme). In both cases, injection detection can be used to measure the phase (related to optical pathlength) or the amplitude (related to the suffered attenuation) of the incoming signal. Thus, we can use injection detection either to make a feedback interferometer and its variants (displacement by fraction-of-wavelength counts, vibrometer, absolute distance sensor, velocimeter) or to make a weak echo detector (return-loss sensor, optical isolator meter,^{16,17} etc.).

Special features of the feedback arrangement, of relevance in applications, are

1. No optical interferometer external to the source is needed, resulting in a very simple, part-count-saving and compact setup.
2. No alignment is necessary, as the laser itself filters out spatially the spatial mode that interacts with the cavity mode.
3. No stray-light filtering before the photodetector is required—the laser diode monitor photodiode is fully adequate.
4. Except for a (modest) reflectivity loss at the entrance mirror, the detected is always in the quantum regime, at the attainable SNR quantum-limit (this implies, e.g., subnanometer sensitivity in pathlength and better than -80 dB detectable return level).
5. Information is carried by the beam and can be picked up everywhere (also at the remote target location).

*Current affiliation: ENSEEIHT-Laboratoire d'Electronique, Toulouse, France.

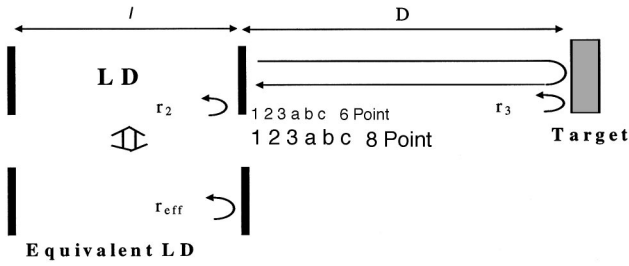


Fig. 1 Equivalent model of an LD with an external target.

Optical feedback interferometry has matured to a well-understood, viable technique for sensing in a variety of applications: (1) displacement measurements with $\lambda/2$ (or better) resolution,^{18–20} (2) absolute (i.e. non-incremental) distance measurements,^{21–23} and (3) velocimetry.^{24,25}

The remarkable advances in both performances and in new instrumental concepts reported in recent years are mainly a consequence of the availability of low-cost, stable and reliable laser diodes, now close to approaching the quality of He-Ne lasers and still improving. As the self-mixing interferometer starts from a very simple setup, room is allowed to aim sophistication, e.g., to satisfy the user's requirement of being able to operate on diffusing target surfaces also, or to drastically reduce costs. Thus, the self-mixing interferometer appears to be very promising for the development of new instruments.

In the following, we describe the theory of the self-mixing effect before discussing some selected measurement applications.

2 Theory of the Self-Mixing Effect

The theory of the self-mixing effect has been extensively analyzed in the literature. There are two alternative and equivalent methods for the analysis: (1) the Lang and Kobayashi set of equations describing the laser in terms of optical and electrical parameters and (2) the three-mirror cavity approach.^{26,27} The former method is more complete and fully accounts for the laser physical parameters, while the latter is much simpler to work out and is correct.

In the following, we use the three-mirror cavity approach and schematize the semiconductor laser diode (LD) with an external target, as in Fig. 1. The front facet of the LD and the external target can be defined by their reflection coefficients r_2 and r_3 , respectively. The optical beam is back-scattered into the LD active cavity (of geometrical length l) by the target, so that the laser operation is affected, causing a substantial variation of the optical output power. To study this disturbance, an equivalent model of this LD with an external target can be introduced.

Concerning the amplitude of the electric field, the complex effective reflection coefficient r_{eff} acts as the reflection coefficient r_2 of the LD with no feedback. Introducing the normalized complex electric field amplitude $E_N(t)$ and including the phase noise due to spontaneous emission,¹⁰ that is:

$$E_N(t) = \sqrt{S(t)} \exp\{j[\phi(t)]\},$$

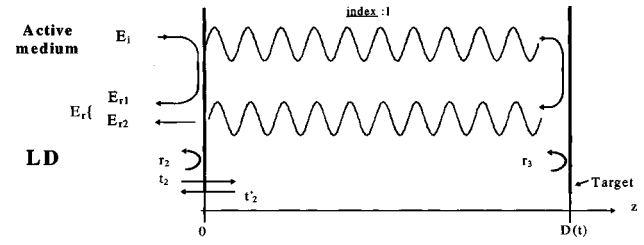


Fig. 2 Electric fields between the LD and the target: E_i is the incident electric field, at $z=0$, E_r, E_{r1} and E_{r2} are the reflecting fields at $z=0$, and t_2, r_2, t_2', r_2' are the transmission and reflection coefficients for the magnitude of the electric field.

where $S(t)$ is the photon number inside the laser cavity, and $\phi(t)$ is the phase, so that:

$$\dot{\phi}(t) = \omega_{cn} - \omega_s,$$

where ω_{cn} is the angular frequency of the electric field with noise and feedback, and ω_s is the angular frequency of the unperturbed electric field.

To simplify the calculations for weak feedback (i.e., $r_3 \ll r_2$), we neglect intensity noise¹⁰ as well as multiple reflection within the external cavity (Fig. 2). The coefficient r_{eff} can then be written as follows:

$$r_{\text{eff}} = \left\langle \frac{E_r}{E_i} \right\rangle = r_2 + (1 - r_2^2) r_3 \frac{\langle E_N(t - \tau_D) E_N^*(t) \rangle}{\langle S \rangle} \exp(-j\omega_s \tau_D), \quad (1)$$

where $t_2 t_2' = 1 - r_2^2$, $\langle X \rangle$ stands for the mean value of X , $\tau_D = (2D)/c$ is the external round trip delay (i.e., the external time of flight) and c is the speed of light in vacuum.

Knowing that a white frequency noise induces a Lorentzian spectrum for the emitted light, the autocorrelation function of the normalized field is given as a function of the spectral width with feedback $\delta\nu_c$:

$$\langle E_N(t) E_N^*(t - \tau_D) \rangle = \langle S \rangle \exp(j\langle \dot{\phi} \rangle \tau_D) \exp(-\pi \delta\nu_c \tau_D). \quad (2)$$

By substituting Eq. (2) in Eq. (1), the effective reflection coefficient that takes into account the influence of the coherent return is given by:

$$r_{\text{eff}} = r_2 [1 + \zeta \exp(-\pi \delta\nu_c \tau_D) \exp(-2\pi \nu_c \tau_D)], \quad (3)$$

where $\zeta = (1 - r_2^2)(r_3/r_2)$ is a parameter denoting the coupling effect from the external reflection back into the LD cavity and $\nu_c = \langle \omega_c \rangle / 2\pi$ is the optical frequency of the emitted light with feedback.

The relationship between $\delta\nu_c$ and the unperturbed spectral width $\delta\nu_s$ is given by²⁶:

$$\delta\nu_c = \frac{\delta\nu_s}{\{1 + C' \cos(2\pi \nu_c \tau_D + \tan^{-1}(\alpha))\}^2}, \quad (4)$$

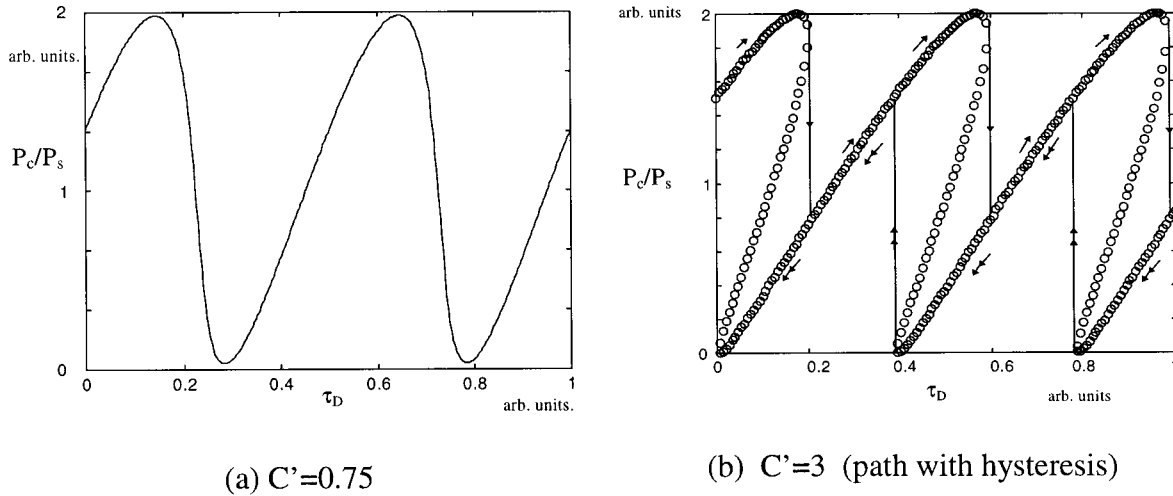


Fig. 3 Theoretical normalized optical power plotted as a function of the external round trip delay. At low feedback (a), the sine wave is somehow distorted; at high feedback (b) hysteresis shows up and the waveform depends on whether target distance is increasing (single arrows) or decreasing (double arrows).

with

$$C' = C \exp(-\pi \delta \nu_c \tau_D),$$

$$C = \frac{\tau_D}{\tau_l} \zeta(1 + \alpha^2)^{1/2},$$

where C' is the modified feedback parameter defining the single mode operation of the LD ($C' < 1$), C is the classical feedback parameter, τ_l is the round trip delay inside the LD active cavity and α is the linewidth enhancement factor.

By solving the equation of stationary laser oscillation for the equivalent LD, the optical frequency ν_c can be written as follows:

$$\nu_c - \nu_s + \frac{C'}{2\pi\tau_D} \sin[2\pi\nu_c\tau_D + \tan^{-1}(\alpha)] = 0, \quad (5)$$

where $\nu_s = \langle \omega_s \rangle / 2\pi$ is the unperturbed optical frequency.

When LD properties are considered with and without feedback under steady state operation, the optical power with feedback P_c can be expressed as a function of the optical power without feedback P_s .

$$P_c = P_s [1 + m' \cos(2\pi\nu_c\tau_D)], \quad (6)$$

where $m' \approx \exp(-\pi \delta \nu_c \tau_D)$ is a modulation parameter.

At weak feedback (i.e., $C' < 1$), the LD is strictly operating as a single-mode LD and the optical power as a function of the target distance exhibits no hysteresis [Fig. 3(a)] at the opposite, at higher feedback level ($1 < C' < 4.6$), the LD is still operating as a single-mode laser, but now both optical frequency and power do exhibit hysteresis²⁷ [Fig. 3(b)].

In the following, only the case of $C' < 4.6$ is considered for sensing applications using the self-mixing interference.

3 Application to Displacement Measurement

By driving the LD with a dc injection current i , both optical frequency and output power without target remain constant when no feedback is applied. Nevertheless, the LD is cooled by a Peltier module for safety.

A moving target generates a periodic saw-tooth like optical power fluctuation, the full swing of power corresponding to a half-wavelength displacement ($\lambda/2 \sim 400$ nm) along the laser beam axis:

$$|\Delta(2\pi\nu_c\tau_D)| = 2\pi \Leftrightarrow |\Delta D| = \frac{c}{2\nu_s} = \frac{\lambda_s}{2}. \quad (7)$$

It is then easy to reconstruct the law of motion of this target just by adding, with the proper sign, such $\lambda/2$ displacements.

In Fig. 4, we can see the theoretical diagram of the output optical power produced by a sinusoidal motion of the target. The displacement direction is recovered by the slope of the saw-tooth like signal. A widely held view clearly confirmed by experiment is that the higher the value of C' , the more contrasted is the saw-tooth like power variation.

Figure 5 shows the block diagram of an experimental setup implemented for displacement measurements. A cw ML64110N LD is driven at a constant optical power of 30 mW and a wavelength $\lambda = 785$ nm. A sine wave generator is used to move the target, which is placed at an average distance D from the LD.

Directional discrimination of this self-mixing interference waveform is obtained by changing the motion direction of the target as clearly confirmed by the shape of the curve on the experimental observation (Fig. 6) showing up and down switchings as the target approaches or moves away from the laser.

By an appropriate signal processing, a resolution of $\lambda/12$ (~ 70 nm) has been obtained for displacements up to several micrometers even in the case of strong hysteresis²⁸

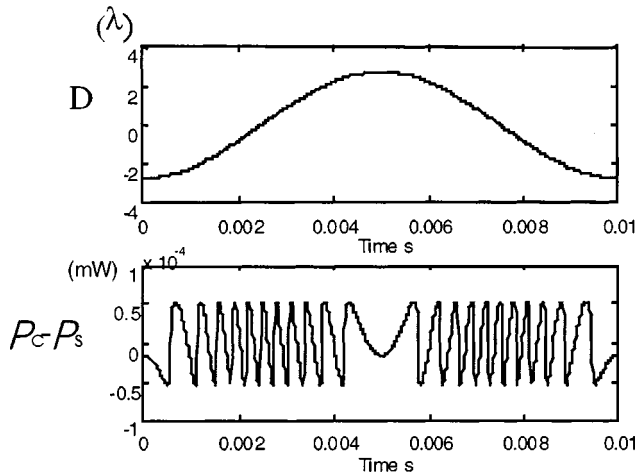


Fig. 4 Optical power variations caused by a sinusoidal motion of the target at an average distance of 20 cm. The frequency is 100 Hz and the amplitude peak to peak is of 5.5λ .

(i.e., high feedback level). This sensor is also suitable to detect resonance frequencies with an accuracy of 0.2 Hz, by applying a fast Fourier transform (FFT) on the reconstructed motion law.²⁹ It has then been shown that this setup is well-suited for the modal analysis of small mechanical parts.

4 Application to Velocity Measurement

The speed of the target, according to the laser beam direction, can be deduced from Eq. (7) by introducing the beat frequency f_b of the saw-tooth like optical power fluctuations:

$$|v_c| = \frac{\lambda_s}{2} f_b. \quad (8)$$

As we can see in Fig. 7(a), the experimental optical-power waveform is strongly altered. This is due to the roughness of the target causing a speckle effect, and makes it difficult to accurately reconstruct the motion law of the target without an appropriate signal processing.

As is well known, when coherent light of the LD is shed on a rough-surface target, the resulting backscattered light presents random intensity and phase distributions and has a granular appearance³⁰—the speckle-pattern noise. A lateral

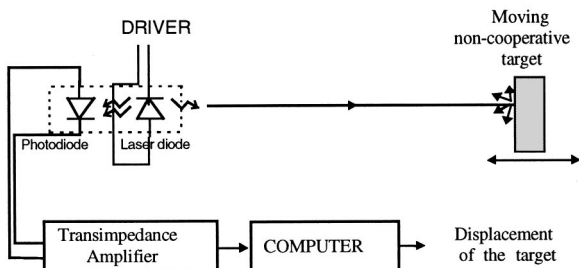


Fig. 5 Block diagram of the experimental setup for displacement measurements.

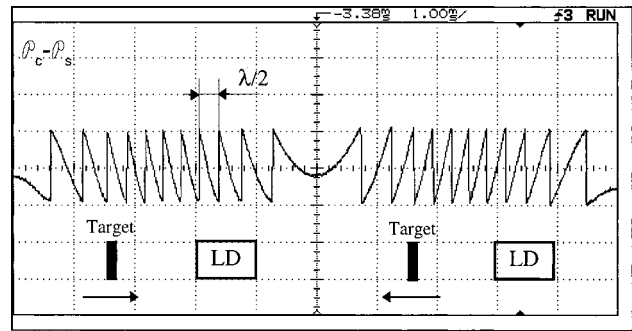


Fig. 6 Experimental observation of the optical power waveform.

displacement of the laser beam on the target also produces an error, because the speckle pattern slides along the LD spatial aperture collecting the signal.

As shown in Fig. 7(b), by means of a real time FFT signal processing directly applied on the saw-tooth like optical power waveform, we were able to determine the beat frequency f_b of the self-mixing signal, so as to calculate the component of the speed of the target parallel to the laser beam axis.

Experimental results on velocity measurements are shown on Fig. 8. For velocities up to 200 km/h, a maximum relative error of 5% has been obtained. This error can also be reduced, by increasing the time constant of integration in the real time FFT signal processing.

5 Application to Vibration Measurements

Locking the interferometric signal to half-fringe, periodic vibrations of amplitude much smaller than the counting step $\lambda/2$ can be resolved, straight in the linear range of response. The ultimate sensitivity is then set by the quantum noise associated to the detected signal, which can be expressed¹⁵ in terms of noise equivalent displacement (NED) as:

$$NED = (\lambda/2\pi) / (SNR),$$

where SNR is the signal-to-noise ratio of the amplitude measurement¹⁵:

$$SNR = (I/2 eB)^{1/2},$$

and I is the detected photocurrent. For example, for $I = 0.01$ mA, we have, from the preceding equations:

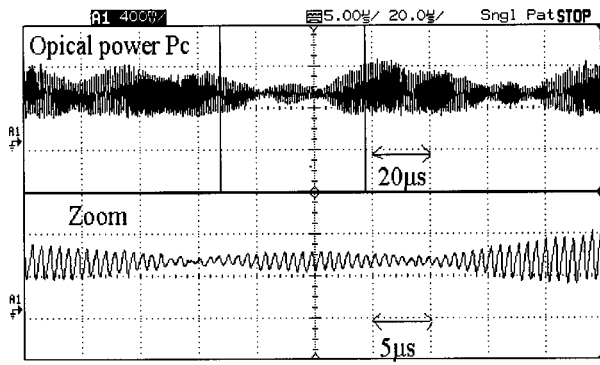
$$NED = (2k)^{-1} (2h\nu B/I)^{1/2} = 0.015 \text{ pm}/\sqrt{\text{Hz}},$$

a remarkable figure indeed. This ultimate level is difficult to achieve, however. Most frequently, the performance is dominated by the preamplifier resistance noise,¹⁵ whose SNR is given by:

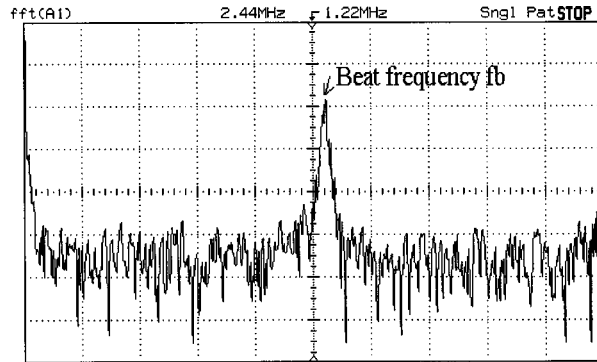
$$SNR = I / (4k_B T B/R)^{1/2},$$

where k_B is the Boltzmann constant, and T is the absolute temperature. Then we get, for a 10-k Ω feedback resistance:

$$NED = (2k)^{-1} (4k_B T B/R)^{1/2} / \sigma P = 0.35 \text{ pm}/\sqrt{\text{Hz}}.$$



(a) Experimental out put power P_c



(b) FFT modulus of the optical output power P_c

Fig. 7 Velocity determination from saw-tooth like power waveform altered by the speckle effect.

Using the self-mixing interferometry on a normal (diffuser or Lambertian) surface, that is, in the speckle-pattern regime, is much easier than a displacement interferometer. Indeed, if we are to detect a very small vibration we shall be able to firmly locate the instrument in front of the surface under test, and, if we unluckily fall on a weak-intensity speckle, we can move the beam a little to find a bright speckle, which will be unaltered during the measurement because of the small dynamic range of amplitude vibrations.

In this way, we may fully exploit the advantages of self-mixing (see points outlined in Sec. 1). An application example is the pickup of the oscillation waveform in a micromachined-electromechanical (MEM) Si-gyroscope,³¹ obtained by an LD at a 50-cm distance from a glass vacuum-tight chamber, with the beam simply focalized onto the comb-like MEM structure. The advantage of the method is that no spatial filtering is required; only the moving parts contribute to the ac signal out from the photodiode (again, the monitor device of the LD), and operation in ambient light, as well as with no special glass window is obtained.

6 Application to Distance Measurement

Absolute distance measurement has been developed with the self-mixing interferometer, using a pulsed-scheme cor-

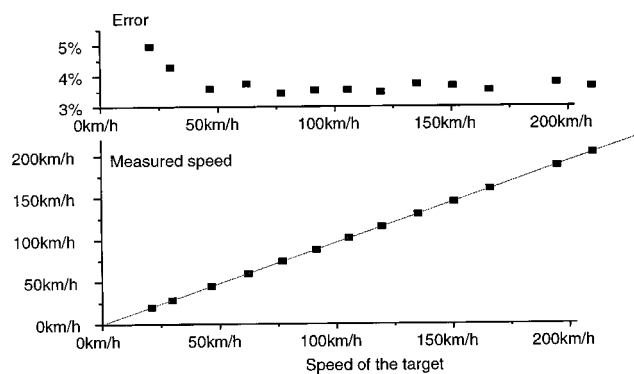


Fig. 8 Experimental calibration of velocity measurement.

responding to make the derivative of optical power waveform.³² Distance to the target can then be expressed by the classical approximate relationship:

$$D \approx \frac{c}{4\Delta\nu} (\sigma_0 N_{b0} + \sigma_1 N_{b1}), \quad (9)$$

where N_{b1} and N_{b0} are, respectively, the integer number of pulses recorded during the upward and downward optical-power ramp and c is the speed of light (Fig. 9); σ_0 and σ_1 are equal to ± 1 according to the motion of the target.

Such a simple pulse-counting method is adequate to carry out the preliminary demonstration of the experiment. In this case, the resolution of the sensor is directly proportional to the optical frequency shift. Using a state-of-the-art multielectrode distributed Bragg reflector (DBR) structure, continuously tuneable up to 375 GHz, we were able to obtain an accuracy of 0.5 mm at 60 cm (Ref. 33) as compared to the 4 mm of a typical Fabry-Pérot LD 64110N with a 36-GHz optical frequency shift (and no mode hop).

However, the exact relationship giving distances is the following³²:

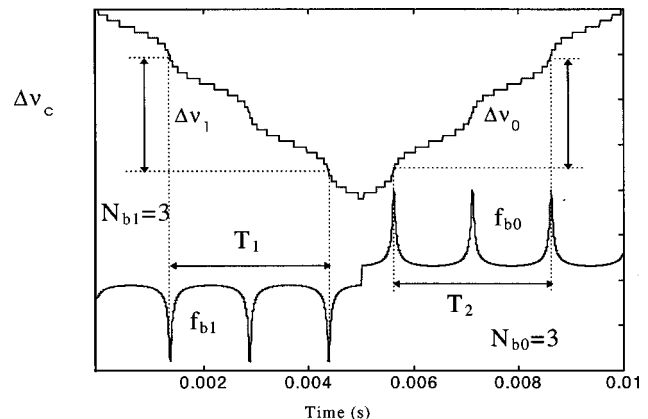


Fig. 9 Optical frequency shift altered by the feedback and the corresponding derivative of the power waveform.

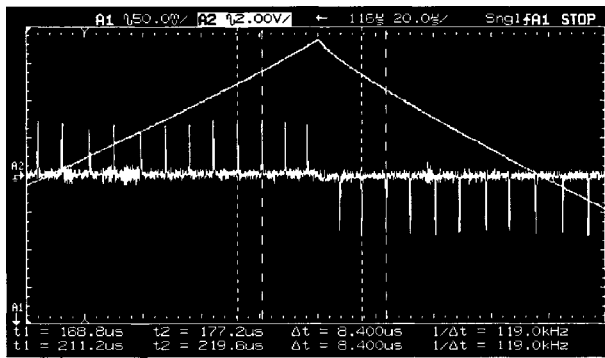


Fig. 10 Reshaped injection current and the derivative of optical power waveform.

$$D = \frac{c}{4(d\nu/dt)} (\sigma_0 f_{b0} + \sigma_1 f_{b1}), \quad (10)$$

where f_{b1} and f_{b0} are the beat frequencies of the output power with feedback, during the upward and the downward ramp, respectively (Fig. 9). Injection current is then modulated by a predistorted triangular signal to make the optical frequency sweep $\Delta\nu$ linear, because the accuracy on distance measurement depends on the stability of both the derivative of the optical frequency and of the beat frequencies on a modulation period. With such a predistorted current, the influence of the thermal time constant on the LD active cavity can be neglected.

Figure 10 shows an oscilloscope display obtained with a Mitsubishi single-mode ML64110N LD with an optical frequency sweep $\Delta\nu = 36$ GHz and a target at rest. An error of roughly 10% in the beat-frequency measurement is corrected, relative to the use of a triangular injection current.³² The maximum error of the distance measurement is then $c/(2\Delta\nu)$ from Eq. (9).

Figure 11 shows that, in the case of the modulated 64110N LD, this maximum error corresponds theoretically to 4.16 mm with Eq. (9) and only to 0.5 mm with Eq. (10). This result is worth considering in the perspective of designing a low-cost range finder with an accuracy equivalent to that obtained with the DBR source. Experimentally, several possible causes for discrepancy from the ideal performance have been analyzed.³⁴ Currently, an experimental accuracy of ± 1.5 mm for a range of 1 to 2 m has been attained (Fig. 12).

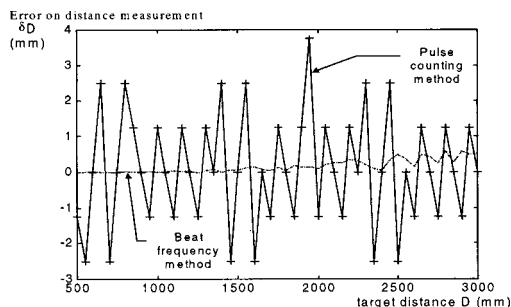


Fig. 11 Comparison between the pulse counting method and the beat frequency measurement.

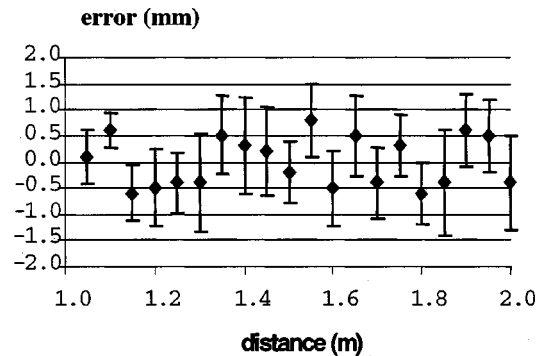


Fig. 12 Calibration of the range finder using the beat frequency measurement.

7 Application to Angle Measurement

When the distance from the LD to the remote target is progressively increased, first we get a high C value and a multistability regime in which the power waveform exhibits several switchings in a $\lambda/2$ period, then we enter in the coherence-collapse regime.¹⁰ Surprisingly, however, a useful detected signal is still obtained, even at a distance $D > L_{\text{coh}}$ larger than the coherence length. This is because, even though incoherent, the addition of a signal in the laser cavity actually eases the oscillation of the laser, or is equivalent to decrease the output mirror reflectivity. The output signal now has an amplitude modulation proportional to the superposition integral of the unperturbed laser field and of the returning field spatial distribution (wider than the mode because of propagation).

If we put a remote reflecting mirror tilted by an angle α respect to the impinging wave vector, then a quadratic dependence $P \approx P_0 [1 + \kappa(\alpha/\alpha_0)^2]$ is found, where κ and α_0 are constants of the experiment.

The quadratic dependence, of course, is not the most desirable dependence for a linear measurement or a high-resolution null measurement near $\alpha = 0$. As explained in another paper in this issue,³⁵ it is easy to get a linear output by adding a minute angular tilt modulation $\Delta\alpha = \Delta\alpha_0 \cos \omega_0 t$ of the mirror-target and phase-lock detecting the power component at the drive frequency ω_0 . By doing so, we obtained an angular resolution of the instrument, operated as an autocollimator, down to a few tenths of arc-second as well as a linearized range (with sign) of angle measurement from $\alpha = -1$ to $+1$ arcmin.

8 Other Applications of the Self-Mix Concept

As noted in the introduction, the self-mix arrangement is also useful to perform a high-sensitivity detection of external signals, either at the same frequency (injection homodyne) or at a slightly different frequency (injection heterodyne) of the unperturbed laser line.

For example, in a narrow-line laser protected by an optical isolator assembled in the laser package, it is very difficult to make a conventional measurement of the isolation factor. Using the self-mixing signal developed by a mirror, purposely aimed to send back a reflection in the cavity, and put in slight vibrations so as to easily detect the fundamen-

tal note on a carrier, it has been shown¹⁶ that the even very effective isolations can be measured, down to -80 to -90 dB the laser power.

Another variant of the same concept is the measurement of return loss of a device under test, inserted between the laser and a final mirror, again put into minute vibration to facilitate signal recovery. Interestingly, as the detection is coherent, the electrical signal obtained from the photodiode decreases by a decade for a 2-decade power decrease (or, of attenuation increase), rendering the method very sensitive³⁶ (again, with a practical limit at -80 to -90 dB).

Last, physical parameters of the laser can be measured by injection interferometry. One reported application is the linewidth $\Delta\nu$ measurement, performed by observing the increasing switching time-jitter τ_j that the interferometric waveform with $C \approx 1$ exhibits when the distance D to the remote reflector is increased. Note that from the slope of the τ_j versus D diagram, the linewidth $\Delta\nu$ is easily found using a distance D considerably shorter than the coherence length.^{37,38}

9 Conclusion

The theory and applications of self-mixing interferometers were summarized. A displacement sensor with a basic resolution of $\lambda/2$ (roughly 400 nm, with single-mode LD ML64110N) was discussed. The sensor was used for velocity measurement by applying an FFT directly to the self-mixing signal to reduce the influence of the speckle. For velocities up to 200 km/h, a maximum relative error of 5% was reached.

A range finder based on the determination of the beat frequencies of optical power variations was designed to improve the accuracy of laser distance measurements. It was calibrated to measure distances from 1 to 2 m with an accuracy of ± 1.5 mm, by reshaping the triangular injection current to remove the influence of thermal effect. Last, we have briefly reported on amplitude-related measurements by self-mixing, such as angle, attenuation, and linewidth.

In conclusion, the self-mixing technique is a very powerful tool in physics and engineering, providing for prospective new unparalleled applications.

References

1. M. B. Spencer and W. E. Lamb, Jr., "Laser with a transmitting window," *Phys. Rev. A* **5**, 884–897 (1972).
2. M. B. Spencer and W. E. Lamb, Jr., "Laser with an external injected signal," *Phys. Rev. A* **5**, 898–912 (1972).
3. C. J. Buczek, R. J. Freiberg, and M. L. Skolnick, "Laser injection locking," *Proc. IEEE* **61**, 1411–1431 (1973).
4. S. Kobayashi and T. Kimura, "Injection locking in semiconductor laser," *IEEE J. Quantum Electron.* **QE-17**, 681–689 (1981).
5. R. Lang, "Injection locking properties of a semiconductor laser," *IEEE J. Quantum Electron.* **QE-18**, 976–983 (1982).
6. V. Annovazzi-Lodi and S. Donati, "Feedback and injection effects in lasers," *IEEE J. Quantum Electron.* **QE-16**, 859–865 (1980).
7. F. Aronowitz, "The laser gyro," in *Laser Applications*, M. Ross, Ed., pp. 134–197, Academic Press, (1971).
8. O. Hirota and Y. Suematsu: "Noise properties of injection lasers due to reflected waves," *IEEE J. Quantum Electron.* **QE-15**, 142–149 (1979).
9. K. Otsuka and S. Tarucha, "Injection locking and injection-induced modulation of laser diodes," *IEEE J. Quantum Electron.* **QE-17**, 1515–1520 (1981).
10. K. Petermann, *Laser Diode Modulation and Noise*, Kluwer Academic, Dordrecht (1988).
11. M. J. Rudd, "A laser Doppler velocimeter employing the laser as a mixer-oscillator," *J. Sci. Instrum.* **1**, 723–726 (1968).
12. A. Seko et al., "Self-quenching in semiconductor lasers and applications to optical memory readout," *Appl. Phys. Lett.* **27**, 140–141 (1975).
13. S. Donati, "Laser interferometry by induced modulation of the cavity field," *J. Appl. Phys.* **49**, 495–497 (1978).
14. P. J. de Groot and G. M. Gallatin, "Three-dimensional imaging coherent laser radar array," *Opt. Eng.* **28**(4), 456–460 (1988).
15. S. Donati, *Photodetectors, Devices, Circuits and Applications*, Chapter 8, Prentice Hall, Upper Saddle River, NJ (2000).
16. S. Donati and M. Sorel, "A phase-modulated feedback method to test optical isolators assembled into the laser package," *IEEE Photonics Technol. Lett.* **PTL-8**, 405–407 (1996).
17. G. Giuliani and S. Donati, "Analysis of the signal amplitude regimes in injection detection," in *Proc. ODIMAP II*, 2nd IEEE-LEOS Topical Meet. on Optoelectronic Distance Measurements and Applications, pp. 75–80, Pavia, Italy (1999).
18. S. Donati, L. Falzoni, and S. Merlo, "A PC-interfaced, compact laser diode feedback interferometer for displacement measurements," *IEEE Trans. Instrum. Meas.* **45**(6), 942–947 (1996).
19. P. A. Roos, M. Stephens, and C. E. Wieman, "Laser vibrometer based on optical-feedback induced frequency modulation of a single-mode laser diode," *Appl. Opt.* **35**(34), 6754–6761 (1996).
20. S. Merlo and S. Donati, "Reconstruction of displacement waveforms with a single-channel laser diode feedback interferometer," *IEEE J. Quantum Electron.* **33**(4), 527–531 (1997).
21. G. Beheim and K. Fritsch, "Range finding using frequency-modulated laser diode" *Appl. Opt.* **25**, 1439–1442 (May 1986).
22. S. Shinohara, H. Yoshida, H. Ikeda, K. Nishide, and M. Sumi, "Compact and high-precision range finder with wide dynamic range and its application," *IEEE Trans. Instrum. Meas.* **41**, 40–44 (Feb. 1992).
23. P. J. de Groot, G. M. Gallatin, and S. H. Macomber, "Ranging and velocimetry signal generation in a backscatter-modulated laser diode," *Appl. Opt.* **27**, 4475–4480 (Nov. 1988).
24. T. Shibata, S. Shinohara, H. Ikeda, H. Yoshida, T. Sawaki, and M. Sumi, "Laser speckle velocimeter using self-mixing laser diode," *IEEE Trans. Instrum. Meas.* **45**(2), 499–503 (1996).
25. W. M. Wang, K. T. V. Grattan, A. W. Palmer, and W. J. O. Boyle, "Self-mixing interference inside a single-mode diode laser for optical sensing applications," *J. Lightwave Technol.* **12**, 1577–1587 (Sep. 1994).
26. G. Mourat, N. Servagent, and T. Bosch, "Optical feedback effects on the spectral linewidth of semiconductor laser sensors using the self-mixing interference," *IEEE J. Quantum Electron.* **34**(9), 1717–1721 (1998).
27. S. Donati, G. Giuliani, and S. Merlo, "Laser diode feedback interferometer for measurement of displacements without ambiguity," *IEEE J. Quantum Electron.* **31**(1), 113–119 (1995).
28. N. Servagent, F. Gouaux, and T. Bosch, "Measurements of displacement using the self-mixing interference in a laser diode," *J. Opt.* **29**(3), 168–173 (1998).
29. N. Servagent, T. Bosch, and M. Lescure, "A laser displacement sensor using the self-mixing effect for modal analysis and defect detection," *IEEE Trans. Instrum. Meas.* **46**(4), 847–850 (1997).
30. J. C. Dainty, Ed., *Laser Speckle and Related Phenomena, Topics in Appl Physics*, Vol. 9, Springer-Verlag, (1984).
31. V. Annovazzi Lodi, S. Merlo, and M. Norgia, "Interferometric characterization of a MEMS gyroscope," *IEEE/ASME Trans. Mechatron.* (in press).
32. F. Gouaux, N. Servagent, and T. Bosch, "Absolute distance measurement with an optical feedback interferometer," *Appl. Opt.* **37**(28), 6684–6689 (1998).
33. G. Mourat, N. Servagent, and T. Bosch, "Distance measurements using the self-mixing effect in a 3-electrode DBR laser diode," *Opt. Eng.* **39**(3), 738–743 (2000).
34. N. Servagent, G. Mourat, F. Gouaux, and T. Bosch, "Analysis of some intrinsic limitations of a laser range finder using the self-mixing interference," *Proc. SPIE* **3479**, 76–83 (1998).
35. G. Giuliani, S. Donati, M. Passerini, and T. Bosch, "Angle measurements by injection detection in a laser diode," *Opt. Eng.*, in this issue.
36. G. Giuliani and S. Donati, "Return loss measurements by feedback interferometry," in *Proc. WFOPC'98, Workshop on Fiber Optics Passive Components*, pp. 103–106, Pavia, Italy (1998).
37. G. Giuliani, M. Norgia, and S. Donati, "Laser diode coherence length measurement by means of self-mixing interferometry," in *Proc. LEOS Ann. Meeting*, pp. 726–727, San Francisco (1999).
38. G. Giuliani and M. Norgia, "Measuring laser diode linewidth by means of injection interferometry," *IEEE Photonics Technol. Lett.* (in press).

Thierry Bosch: Biography and photograph appear with the guest editorial in this issue.

Silvano Donati: Biography and photograph appear with the guest editorial in this issue.



Noël Servagent received his Diplôme d'Etudes Approfondies from the University of Liège, Belgium, and the title of engineer from the School of Mines of Ales, France, in 1992. In 1997, he received his PhD degree in electronics engineering from the National Polytechnic Institute of Toulouse, France. He is currently an assistant professor with the School of Mines of Nantes, France. His research interest is optical measurement techniques, including vibration and distance measurements.